Photocatalytic Properties of RuO2-Loaded β-Ge3N4 for Overall Water Splitting

ARTICLE *in* THE JOURNAL OF PHYSICAL CHEMISTRY C · MARCH 2007

Impact Factor: 4.77 · DOI: 10.1021/jp067254c

Photocatalytic Properties of RuO_2-Loaded β-Ge_3N_4 for Overall Water Splitting

Kazuhiko Maeda,[†] Nobuo Saito,[‡] Daling Lu,[§] Yasunobu Inoue,[‡] and Kazunari Domen*[,†,§]

Department of Chemical System Engineering, The University of Tokyo, 7-3-1 Hongo, Bunkyo-ku, Tokyo 113-8656, Japan, Department of Chemistry, Nagaoka University of Technology, Nagaoka 940-2188, Japan, and Solution Oriented Research for Science and Technology (SORST) programs of the Japan Science and Technology Agency (JST), 4-1-8 Honcho, Kawaguchi-shi, Saitama 332-0012, Japan

Received: November 3, 2006; In Final Form: January 26, 2007

Germanium nitride, β-Ge_3N_4, is studied as a non-oxide photocatalyst for overall water splitting. Nitridation of GeO_2 at 1153 K for 10 h under a flow of NH_3 results in the production of well-crystallized β-Ge_3N_4 particles with a phenacite structure belonging to the hexagonal crystal system. Although the as-prepared β-Ge_3N_4 displays negligible activity for overall water splitting, the material becomes photocatalytically active under ultraviolet (UV) irradiation ($\lambda > 200$ nm) when loaded with RuO_2 nanoparticles as H_2 evolution sites. The photocatalytic activity of RuO_2-loaded β-Ge_3N_4 for overall water splitting is strongly dependent on the reaction conditions. The highest activity is obtained when the reaction is carried out in 1 M H_2SO_4 aqueous solution. The rates of both H_2 and O_2 evolution decreases as the reaction progresses, attributable to photoreduction of O_2, collapse of the catalyst surface by elusion of Ge cations, and loosened interfacial contact between the β-Ge_3N_4 and the loaded RuO_2 nanoparticles. Up to 80% of the initial activity can be recovered by calcination of the used catalyst at 673 K in air for 5 h followed by reloading with RuO_2.

1. Introduction

Overall water splitting using a heterogeneous photocatalyst has been studied extensively for the supply of clean and renewable hydrogen energy on a large scale. The reaction is an "uphill" type reaction involving a large increase in Gibbs energy (238 kJ/mol). A number of metal oxides containing d^0-transition metal cations (e.g., Ti^{4+}, Zr^{4+}, Nb^{5+}, Ta^{5+}, and W^{6+}) or d^{10}-typical metal cations (e.g., Ga^{3+}, In^{3+}, Ge^{4+}, Sn^{4+}, and Sb^{5+}) as principal metal components have been reported to be active photocatalysts for overall water splitting.[1−11] However, the photocatalytic materials identified to date to be capable of splitting water had comprised solely metal oxides, because of the lack of a material that has appropriate band edge positions and adequate stability during the photocatalysis process.

Recently, the present authors presented a brief report on a modification of a typical metal nitride with d^{10} electronic configuration, β-Ge_3N_4, by loading RuO_2 nanoparticles to achieve functionality as a photocatalyst for the stoichiometric decomposition of water under ultraviolet (UV) irradiation ($\lambda >$ 200 nm).[12] This is the first successful example of overall water splitting using a non-oxide photocatalyst. Conventional non-oxide photocatalysts, such as CdS and CdSe, are unable to achieve overall water splitting primarily because of the inherent instability of the S 3p populated valence band in the water oxidation reaction, which involves the production of photogenerated holes.[13] In contrast, density functional theory (DFT) calculations suggest that β-Ge_3N_4 can promote the reaction despite having valence bands populated by N 2p orbitals. It is of interest that the N 2p orbitals are also available for water oxidation (a four-electron process) as well as O 2p orbitals in metal oxide photocatalysts. β-Ge_3N_4 has a phenacite crystal structure consisting of corner-shared GeN_4 tetrahedrons, as shown in Figure 1.

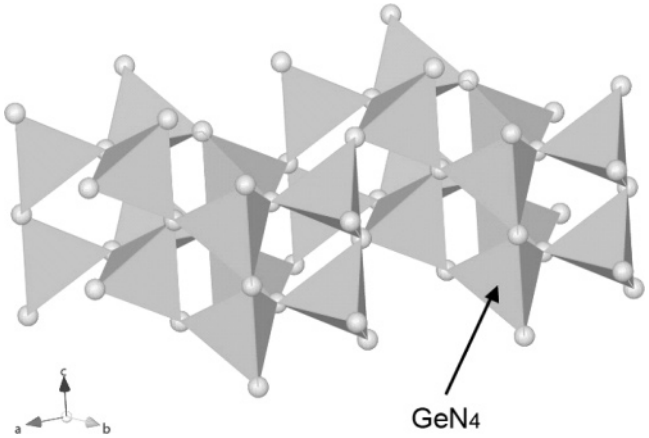

Figure 1. Crystal structure of β-Ge_3N_4.

The discovery of a non-oxide photocatalyst achieving overall water splitting is expected to offer new opportunities for progress in the development of visible-light-driven photocatalysis. The higher valence band position of non-oxide materials (e.g., (oxy)nitrides and oxysulfides) compared to the corresponding metal oxides provides a narrower band gap that is suitable for the visible-light reaction.[14−17] To develop a highly efficient photocatalytic system, it is important to investigate the reaction conditions affecting the activity of a given photocatalyst. However, there are only a few reports describing the effect of reaction conditions on the activity of non-oxide photocatalysts for overall water splitting.[15,16] In a preliminary communication, we presented the overall water splitting on RuO_2-loaded β-Ge_3N_4 under UV irradiation ($\lambda > 200$ nm).[12] The present

* To whom correspondence should be addressed. E-mail: domen@chemsys.t.u-tokyo.ac.jp. Present address: Department of Chemical System Engineering, The University of Tokyo, 7-3-1 Hongo, Bunkyo-ku, Tokyo 113-8656, Japan. Tel.: +81-3-5841-1148. Fax: +81-3-5841-8838.

[†] The University of Tokyo.

[‡] Nagaoka University of Technology.

[§] Japan Science and Technology Agency.

10.1021/jp067254c CCC: $37.00
Published on Web 03/07/2007

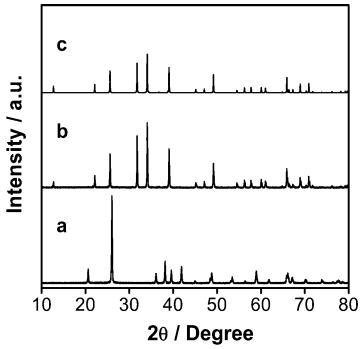

Figure 2. Powder XRD pattern of (a) GeO_2 precursor, (b) product obtained by nitriding GeO_2 powder at 1153 K for 10 h, and (c) β-Ge_3N_4 reference (JCPDS Card No. 38-1374).

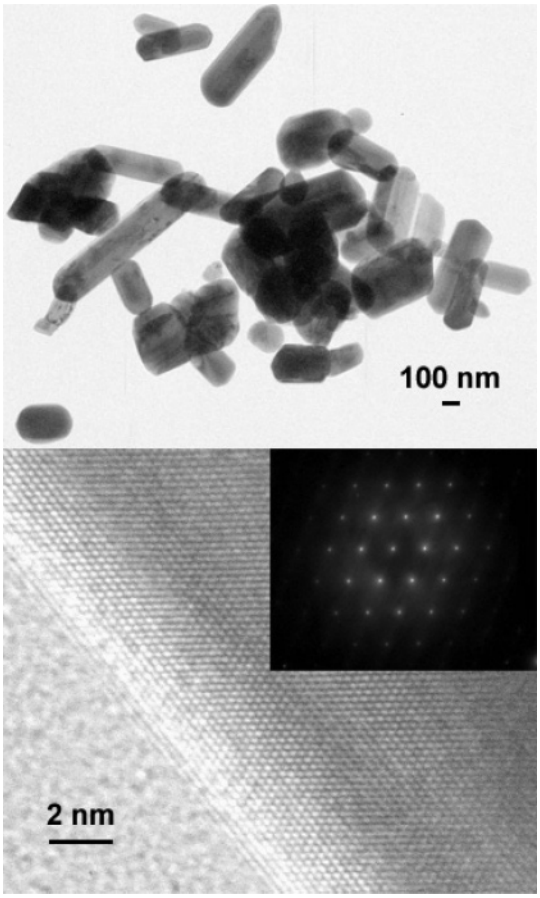

Figure 3. HR-TEM images and electron diffraction pattern of as-prepared β-Ge_3N_4.

article reports on a more detailed investigation of the photocatalytic properties of RuO_2-loaded β-Ge_3N_4 for overall water splitting.

2. Experimental Section

2.1. Preparation of β-Ge_3N_4 and RuO_2 Modification. β-Ge_3N_4 was prepared by heating GeO_2 (99.99%, Kanto Chemicals) powder (ca. 2 g) at 1153 K under NH_3 flow (100 mL/min). After 10 h of nitridation, the sample was cooled to room temperature under NH_3 flow and then ground into a powder.

RuO_2 nanoparticles as a cocatalyst for H_2 evolution were loaded onto the as-prepared β-Ge_3N_4 according to the method presented previously.[2,9−11] Briefly, the β-Ge_3N_4 powder was immersed in a tetrahydrofuran (THF) solution containing

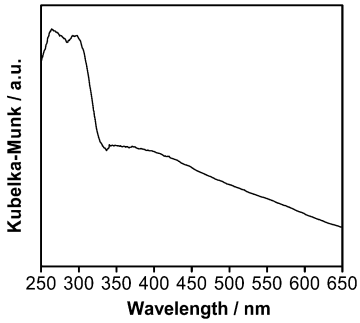

Figure 4. UV−visible DRS spectrum for as-prepared β-Ge_3N_4.

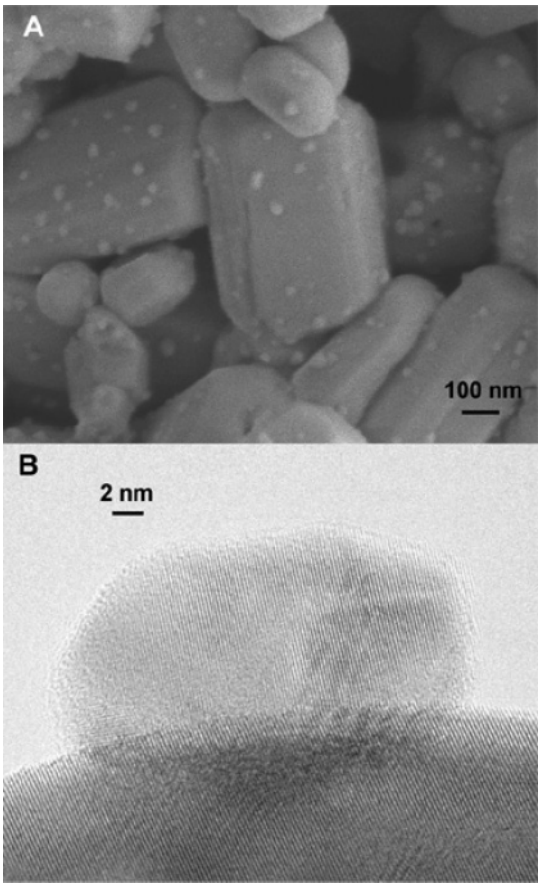

Figure 5. (A) SEM and (B) HR-TEM image of 1 wt % RuO_2-loaded β-Ge_3N_4.

dissolved $Ru_3(CO)_{12}$ (99%, Aldrich Chemical Co.) and stirred at 333 K for 4 h. The solution was then dried under reduced pressure, followed by heating in air at 373 K for 1 h to remove THF. The resulting powder was finally heated in air at 673 K for 5 h to convert the Ru species to RuO_2. RuO_2 was loaded at a rate of 1 wt %.

2.2. Characterization of Catalysts. The prepared samples were studied by powder X-ray diffraction (XRD; RINT2500HR-PC, Rigaku; Cu Kα), high-resolution transmission electron microscopy (HR-TEM; JEM-2010F, JEOL), scanning electron microscopy (SEM; S-4700, Hitachi), UV−visible diffuse reflectance spectroscopy (DRS; V-560, Jasco), and X-ray photoelectron spectroscopy (XPS; ESCA-3200, Shimadzu). The binding energies determined by XPS were corrected in reference to the Au $4f_{7/2}$ peak (83.8 eV) for each sample. The Brunauer−Emmett−Teller (BET) surface area was measured using a Coulter SA-3100 instrument at liquid nitrogen temperature.

2.3. Photocatalytic Reactions. Reactions were typically carried out in a quartz inner-irradiation-type reaction vessel connected to a glass closed gas circulation system. A 0.5 g

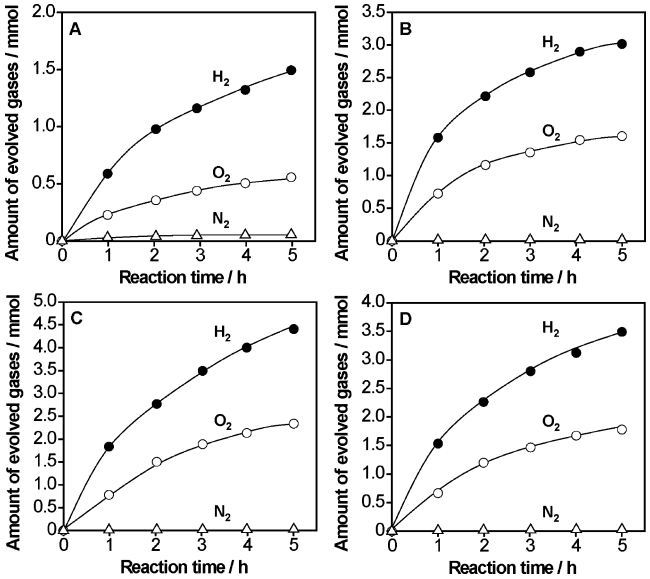

Figure 6. Overall water splitting using 1 wt % RuO_2-loaded β-Ge_3N_4 under UV irradiation (λ > 200 nm) in (A) pure water, (B) aqueous H_2SO_4 solution of 1×10^{-3} M, (C) aqueous H_2SO_4 solution of 1 M, and (D) aqueous H_2SO_4 solution of 2 M. Catalyst (0.5 g); an aqueous H_2SO_4 solution or distilled water (390 mL); light source, high-pressure mercury lamp (450 W); inner irradiation-type reaction vessel made of quartz.

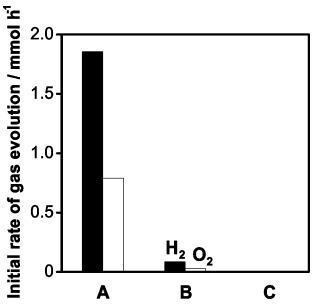

Figure 7. Dependence of photocatalytic activity of 1 wt % RuO_2-loaded β-Ge_3N_4 for overall water splitting on wavelength of incident light: λ > (A) 200, (B) 300, and (C) 400 nm. Catalyst (0.5 g); an aqueous H_2SO_4 solution (1 M, 350−400 mL); light source, high-pressure mercury lamp (450 W); inner irradiation-type reaction vessel made of quartz or Pyrex with or without an aqueous $NaNO_2$ solution (2 M) filter.

sample of the RuO_2-loaded catalyst was dispersed in an aqueous H_2SO_4 solution or distilled water, and the solution was evacuated several times to remove air completely, followed by irradiation (λ > 200 nm) using a 450 W high-pressure Hg lamp (UM-452, Ushio). The temperature of the reactant solution was maintained at 293 ± 5 K by a flow of cooling water during the reaction. The gases evolved in the reaction were analyzed by gas chromatography.

3. Results and Discussion

3.1. XRD, HR-TEM, and UV−Visible DRS. Figure 2 shows the XRD pattern of the product obtained by nitriding GeO_2 powder at 1153 K for 10 h. The pattern for the starting GeO_2 powder is shown for reference. The product exhibits a single-phase diffraction pattern indicative of a phenacite crystal structure, consistent with the β-Ge_3N_4 reference.[18] No diffraction peak assigned to GeO_2 could be identified in the nitridation product, indicating that complete nitridation of the GeO_2 precursor can be achieved under the present nitridation conditions. HR-TEM images and an electron diffraction pattern of

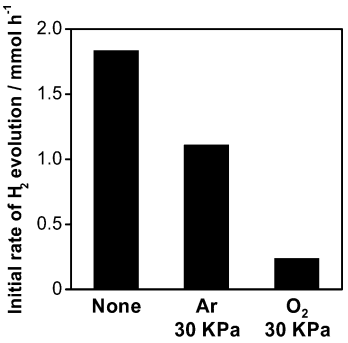

Figure 8. Effect of gases in the reaction system on photocatalytic activity of 1 wt % RuO_2-loaded β-Ge_3N_4 for overall water splitting under UV irradiation (λ > 200 nm). Catalyst (0.5 g); an aqueous H_2SO_4 solution (1 M, 390 mL); light source, high-pressure mercury lamp (450 W); inner irradiation-type reaction vessel made of quartz.

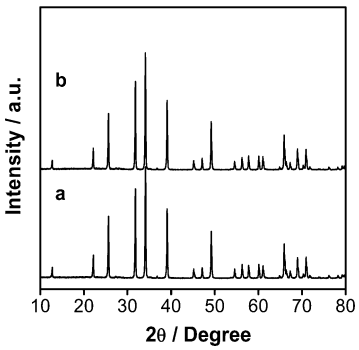

Figure 9. Powder XRD patterns of 1 wt % RuO_2-loaded β-Ge_3N_4 (a) before and (b) after overall water splitting in an aqueous 1 M H_2SO_4 solution for 24 h.

the same sample are shown in Figure 3. These observations revealed the as-prepared β-Ge_3N_4 to consist of primary well-crystallized rod-like particles with a hexagonal crystal system, as indicated by the clear lattice fringes and electron diffraction pattern of the particle. The specific surface area of the as-prepared β-Ge_3N_4 was approximately 2.4 m^2/g.

The UV−visible DRS spectrum for the as-prepared β-Ge_3N_4 is shown in Figure 4. β-Ge_3N_4 produces a sharp absorption around 350 nm, accompanied by a broad absorption in the visible-light region. It has been confirmed by our previous excitation and emission measurements that the absorption around 350 nm originates from the band gap transition.[12,19] As mentioned in a previous paper, DFT calculations show that the tops of the valence bands for β-Ge_3N_4 are composed of N 2p orbitals, whereas the bottoms of the conduction bands consist of 4s,4p hybridized orbitals of Ge.[12] The absorption band around 350 nm is therefore attributable to the transition from N 2p orbitals to hybridized Ge 4s,4p orbitals. The absorption band in the visible light region, on the other hand, is attributable to impurities or defect sites, as mentioned previously.[12,19]

3.2. Photocatalytic Properties. As reported previously, β-Ge_3N_4 alone exhibits almost no photocatalytic activity for water splitting. With RuO_2 modification, however, substantial photocatalytic activity was obtained for simultaneous H_2 and O_2 evolution from pure water. Figure 5 shows SEM and HR-TEM images of the 1 wt % RuO_2-loaded β-Ge_3N_4. The images reveal that RuO_2 nanoparticles of 20−50 nm in size are dispersed uniformly on the β-Ge_3N_4 surface, and the lattice fringes in the TEM image indicate that the loaded RuO_2 nanoparticles are crystalline. Very recently, Shimodaira et al. have investigated the electronic structures of cocatalyst/photocatalyst ($NiO_x/K_2La_2Ti_3O_{10}$) interface used for overall water

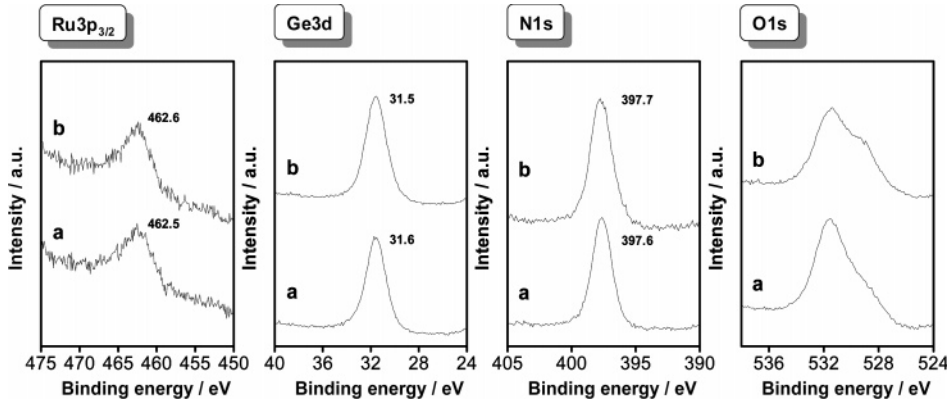

Figure 10. XPS spectra of Ru $3p_{3/2}$, Ge 3d, N 1s, and O 1s peaks for 1 wt % RuO_2-loaded β-Ge_3N_4 (a) before and (b) after overall water splitting in an aqueous 1 M H_2SO_4 solution for 24 h.

TABLE 1: Surface Atomic Ratios of 1 wt % RuO_2-Loaded β-Ge_3N_4 before and after Photocatalytic Reaction

	surface atomic ratio		
sample	Ru/Ge	N/Ge	O[a]/Ge
before reaction	0.05	1.2	1.0
after reaction for 24 h	0.06	1.4	0.8

[a] Estimated from the areas of entire O 1s peak and Ge 3d.

splitting by the two-dimensional surface model DFT calculations.[20] According to that study, it has been claimed that a mixing between Ni 3d and Ti 3d orbitals in $NiO_x/K_2La_2Ti_3O_{10}$ is responsible for the electron transfer from $K_2La_2Ti_3O_{10}$ to NiO_x playing an essential role in overall water splitting. In the present RuO_2/β-Ge_3N_4 system, it is therefore expected that the electron transfer from β-Ge_3N_4 to RuO_2 takes place through a similar mechanism to the $NiO_x/K_2La_2Ti_3O_{10}$ system and that the loaded RuO_2 nanoparticles on the β-Ge_3N_4 surface function as reduction sites for H^+ into H_2 by the photogenerated electrons. The idea that RuO_2 nanoparticles dispersed on β-Ge_3N_4 act as a reduction catalyst for H_2 evolution is in agreement with the previous studies.[2,16]

The photocatalytic activity of the RuO_2-loaded β-Ge_3N_4 for overall water splitting was found to be strongly dependent on the H_2SO_4 concentration of the reactant solution. Figure 6 shows the time courses of overall water splitting on the RuO_2-loaded β-Ge_3N_4 under UV irradiation ($\lambda > 200$ nm) in solutions of various H_2SO_4 concentrations. The reproducibility of the rate of H_2 and O_2 evolution in the overall water splitting was within ~15% under the same reaction conditions. Both H_2 and O_2 evolved in all cases, but the rates of both H_2 and O_2 evolution decreased with reaction time. The reason for this deactivation will be discussed later. In pure water, the rate of O_2 evolution was lower than that expected from the stoichiometry. Furthermore, a relatively high level of N_2 evolution was observed continuously in the reaction, indicating that the material is gradually decomposed by photogenerated holes. This decomposition consumes photogenerated holes that would otherwise be consumed in the oxidation of water and is described as follows.

$$2N^{3-} + 6h^+ \rightarrow N_2$$

However, as the concentration of H_2SO_4 was increased (up to 1 M), the rate of H_2 and O_2 evolution became stoichiometric and increased. At H_2SO_4 concentrations exceeding 1 M, the evolution rates began to degrade. N_2 evolution, indicative of the partial decomposition of the nitride photocatalyst, was also increasingly suppressed at higher H_2SO_4 concentrations. When a solution containing 1 M H_2SO_4 was used, with which the highest photocatalytic performance was obtained, the total H_2 and O_2 evolution over 5 h of reaction (6.7 mmol) was substantially greater than the amount of catalyst employed (0.5 g; 1.8 mmol of β-Ge_3N_4), providing confirmation of the catalytic cycle. It appears that the enhanced activity of RuO_2-loaded β-Ge_3N_4 with increasing H_2SO_4 concentration is associated with the suppression of hydrolysis. In general, (oxy)nitride materials are inherently unstable in basic media as a result of hydrolysis of the material but are stable in acidic media. For example, it has been reported that RuO_2- or $Rh_{2-y}Cr_yO_3$-loaded $(Ga_{1-x}Zn_x)$-$(N_{1-x}O_x)$ photocatalysts exhibit higher activity for overall water splitting in acidic media than in neutral or basic media and that the $Rh_{2-y}Cr_yO_3$-loaded counterpart suspended in neutral media undergoes gradual hydrolysis-induced deactivation.[15,16] Such hydrolysis takes place on the catalyst surface, resulting in the direct deactivation of active sites. Another possible explanation for the improvement is the promotion of water reduction ($2H^+ + 2e^- \rightarrow H_2$) due to an increase in H^+ concentration with the addition of H_2SO_4. Increasing the H_2SO_4 concentration above 1 M has the effect of reducing activity, possibly a result of the detrimental effect of such high H^+ concentrations on the water oxidation reaction ($2OH^- + 4h^+ \rightarrow O_2 + 2H^+$). It should be noted that this characteristic pH dependence of the RuO_2-loaded β-Ge_3N_4 photocatalyst deviates significantly from the general character of metal oxide photocatalysts.[1b,7]

Figure 7 shows the dependence of the photocatalytic activity of RuO_2-loaded β-Ge_3N_4 for overall water splitting on the wavelength of incident light, which was controlled in the reaction by inserting quartz or Pyrex vessels with or without aqueous $NaNO_2$ solution (2 M) in the light path as a wavelength filter.[15,16] The rate of H_2 and O_2 evolution in overall water splitting decreased with increasing the wavelength of the incident light, as a result of a decrease in the number of incident photons from the light source. No H_2 and O_2 evolution was observed when the reaction was carried out at wavelengths longer than 400 nm or in the dark. These results indicate that the sharp absorption band at 350 nm (Figure 4), indicative of the band gap transition from the valence band formed by N 2p orbitals to the conduction band formed by Ge 4s,4p hybridized orbitals, contributes to promoting overall water splitting on RuO_2-loaded β-Ge_3N_4. In addition, it is clear that the broad absorption in the visible-light region (Figure 4) assignable to impurities and/or defect sites is not available for the reaction.

3.3. Reason for Deactivation. It is important to clarify the factors affecting deactivation of the photocatalyst upon reaction

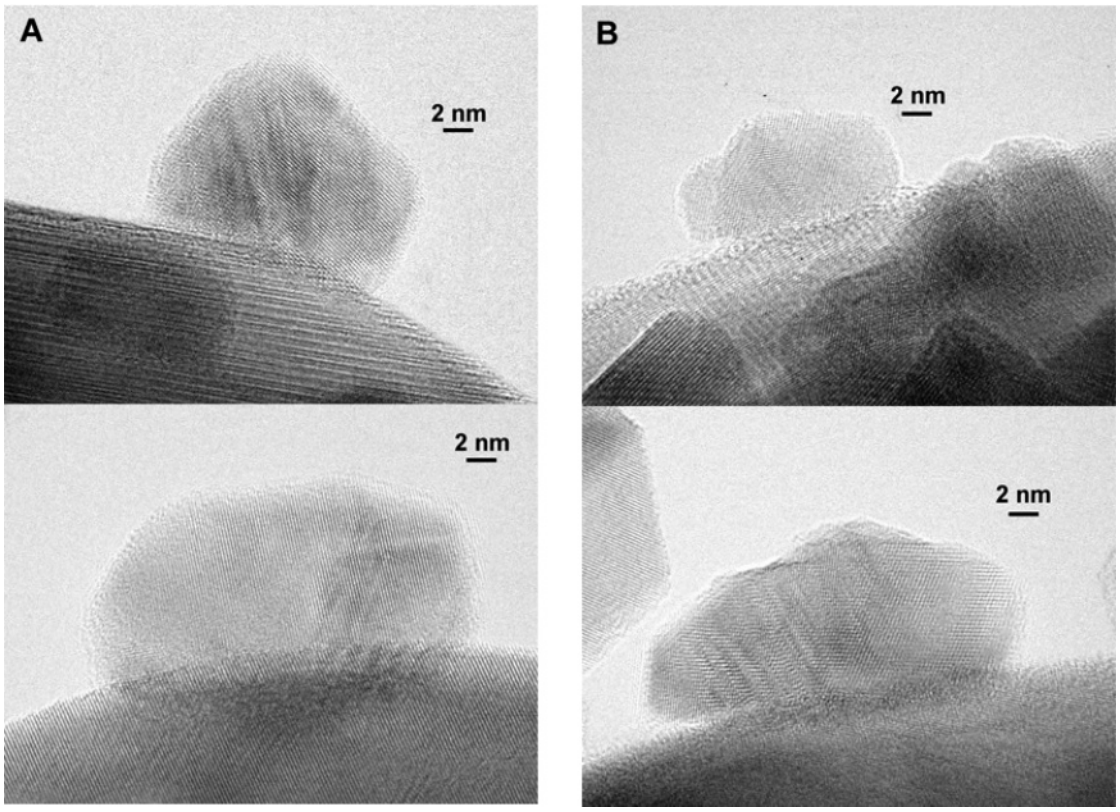

Figure 11. HR-TEM images of 1 wt % RuO_2-loaded β-Ge_3N_4 (A) before and (B) after overall water splitting in an aqueous 1 M H_2SO_4 solution for 24 h.

to develop an efficient photocatalytic system. In the present case, the rates of both H_2 and O_2 evolution decrease as the reaction progresses, regardless of the concentration of H_2SO_4, as shown in Figure 6. It is known that the gaseous pressure, particularly of O_2, in the reaction system affects the photocatalytic activity for overall water splitting. For example, the photocatalytic activity of NiO-loaded $SrTiO_3$,[2c] Pt-loaded TiO_2,[3] ZrO_2,[4] and RuO_2-loaded $(Ga_{1-x}Zn_x)(N_{1-x}O_x)$[16] has been reported to be suppressed in the presence of gaseous oxygen. The effect of gases in the reaction system on the photocatalytic activity of RuO_2-loaded β-Ge_3N_4 was therefore examined in more detail. Figure 8 shows the rate of H_2 evolution in overall water splitting using RuO_2-loaded β-Ge_3N_4 in the presence of various gases. The introduction of Ar gas (30 kPa) into the reaction system before irradiation suppressed the photocatalytic activity of the RuO_2-loaded sample by about 60%, which can be explained as due to the effect of gas pressure. The introduction of O_2 gas (30 kPa) had an even more pronounced suppression effect. It is thus clear that the activity of the RuO_2-loaded β-Ge_3N_4 is suppressed by the effects of gas pressure and O_2, suggesting that photoreduction of O_2[2c,3,4,16] occurs on the RuO_2-loaded β-Ge_3N_4 catalyst during the overall water splitting reaction. If activity suppression by gaseous oxygen is the primary cause of the deactivation observed in the reaction, the activity should be recoverable by evacuation of the reaction system. However, as presented in the preliminary communication, the activity of the RuO_2-loaded β-Ge_3N_4 does not recover in this way,[12] indicating that irreversible deactivation of the catalyst occurs in the overall water splitting reaction.

Catalysts reacted for 24 h in an aqueous 1 M H_2SO_4 solution were characterized by XRD, XPS, and HR-TEM. The XRD patterns of the samples before and after the reaction (Figure 9) show that the crystal structures of the samples were essentially unchanged by the reaction. Figure 10 shows the XPS spectra for Ru $3p_{3/2}$, Ge 3d, N 1s, and O 1s before and after the reaction. Although the photoelectron signal of Ru 3d appears much stronger than that of Ru 3p, the Ru 3d photoelectron signal overlaps the C 1s photoelectron signals. Although the peak positions of Ru $3p_{3/2}$, Ge 3d, and N 1s in the used catalyst were not noticeably different from those for the fresh catalyst, the shape of the O 1s spectrum was clearly changed by the reaction. The nature of the change appears to be complex, involving the mixing of various oxygen species derived from the loaded RuO_2, the β-Ge_3N_4 surface, and the adsorbed water molecules, preventing meaningful interpretation of the O 1s spectra. Nevertheless, it can be concluded that the crystal structure and the valence state of the catalyst are largely unchanged by the photocatalytic reaction.

In contrast, the surface atomic compositions of the catalyst underwent distinct changes upon reaction. Table 1 shows the surface atomic ratios (Ru/Ge, N/Ge, and O/Ge) of samples before and after the photocatalytic reaction. The compositions were estimated from the areas of the corresponding XPS peaks shown in Figure 10. Although the Ru/Ge ratio did not change upon reaction, the N/Ge and O/Ge ratios increased and decreased, respectively. In most cases, the nitrogen/metal atomic ratio of the (oxy)nitride-type material decreases upon photocatalytic reaction because of the release of a small amount of N_2 in the initial stage of the reaction.[16] Taking this N_2 release into account (observed experimentally), the increase in the N/Ge ratio upon reaction is expected to be due to a decrease in the density of surface Ge species. As expected, inductively coupled plasma (ICP) mass spectrometry revealed that the solution contained approximately 7.5 mg of Ge cations and no Ru cations after the reaction. It is thus considered that the increase in the N/Ge ratio upon reaction is mainly due to elution of the surface

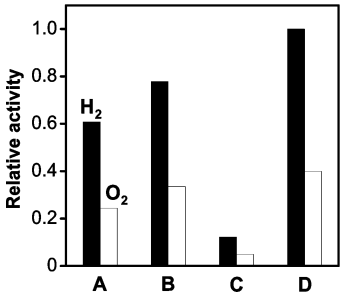

Figure 12. Second-run photocatalytic activities of 1 wt % RuO_2-loaded β-Ge_3N_4 after treating the first-run catalysts by (A) heat treatment at 673 K for 5 h in air, (B) reloading with 1 wt % RuO_2 by the standard method, and (C) without regenerative treatment. (D) Photocatalytic activity of fresh catalyst. Catalyst (0.15 g); an aqueous H_2SO_4 solution (1 M, 390 mL); light source, high-pressure mercury lamp (450 W); inner irradiation-type reaction vessel made of quartz.

Ge cations. Since GeO_2 is slightly soluble in aqueous media,[21] Ge−O species on the β-Ge_3N_4 surface are presumably eluted from the photocatalyst during the reaction. This is consistent with the decrease in the O/Ge ratio upon reaction (Table 1). Despite this elution of surface Ge cations, the Ru/Ge ratio remained largely unchanged by the reaction, attributable to the relatively low atomic ratio of Ru/Ge in the sample. That is, even though the Ge concentration on the surface decreases to some extent upon reaction, the Ru/Ge ratio does not change noticeably.

Figure 11 displays the HR-TEM images of the interface between β-Ge_3N_4 and the loaded RuO_2 nanoparticles (A) before and (B) after the reaction. Before the reaction, the surface of β-Ge_3N_4 was smooth, and β-Ge_3N_4 and the loaded RuO_2 nanoparticle were well-contacted with each other. However, the surface structure became rougher to some extent after the reaction, which is attributed to elution of the surface Ge cations. This situation would give rise to partial collapse and relaxing the interfacial structure between β-Ge_3N_4 and the loaded RuO_2 nanoparticles. This loosening of the structure hinders prompt electron migration from the β-Ge_3N_4 to the RuO_2, thereby resulting in deactivation of the catalyst.

3.4. Regeneration of Used Catalyst. On the basis of the results above, it is considered that the deactivation observed in overall water splitting on RuO_2-loaded β-Ge_3N_4 is caused by photoreduction of O_2 and elution of surface Ge cations. Such deactivation may be recovered by applying an appropriate form of regeneration treatment to the used catalyst. The used catalyst (reacted in an aqueous 1 M H_2SO_4 solution for 24 h) was filtered and dried in an oven at 343 K overnight, and then divided into three samples to examine different regeneration treatments. One sample was simply heated in air at 673 K for 5 h, another was reloaded with 1 wt % RuO_2 nanoparticles by the standard method, and the last sample remained untreated.

Figure 12 shows the relative activities of the heated, reloaded, and untreated samples for overall water splitting (second reaction). Data for the fresh catalyst are also shown for comparison. The untreated catalyst exhibited activity corresponding to only 12% of that achieved by the fresh catalyst, whereas the heated catalyst recovered 60% of the original activity. The reloaded catalyst displayed even higher recovery of activity. These regenerative enhancements of activity are considered to be attributable to improvement of both electron transfer from the β-Ge_3N_4 to the loaded RuO_2 nanoparticles and an increase in the density of active sites for H_2 evolution. It is thus clear that facilitating electron transfer from the β-Ge_3N_4 to the loaded RuO_2 nanoparticles is crucially important to obtaining high photocatalytic activity in this catalytic system. To the best of the authors' knowledge, such behavior has not been observed for metal oxide-based photocatalysts. In the case of non-oxide photocatalysts, the interfacial properties between the catalysts and the cocatalyst appear to be important and differentiate the non-oxide systems from the metal oxide systems, reflecting the unique photocatalytic properties of nitride photocatalysts.

4. Conclusion

The photocatalytic activity of RuO_2-loaded β-Ge_3N_4 for overall water splitting was shown to be strongly dependent on the H_2SO_4 concentration of the reactant solution and the pressure of gaseous oxygen. In overall water splitting by RuO_2-loaded β-Ge_3N_4, β-Ge_3N_4 absorbs photon energy greater than the band gap, generating electrons and holes in the conduction and valence band, respectively. The conduction band electrons are injected into RuO_2 nanoparticles to reduce adsorbed H^+ into H_2, whereas holes in the valence band oxidize H_2O into O_2 on the surface of β-Ge_3N_4. However, a part of photogenerated electrons are consumed by reduction of O_2 without participating in H_2 evolution reaction. More efficient electron transfer from the β-Ge_3N_4 to the loaded RuO_2 nanoparticles is concluded to be necessary to obtain high photocatalytic activity.

Acknowledgment. This work was supported by the Solution Oriented Research for Science and Technology (SORST) program of the Japan Science and Technology (JST) Agency and the 21st Century Center of Excellence (COE) program of the Ministry of Education, Culture, Sports, Science and Technology of Japan.

References and Notes

(1) (a) Domen, K.; Naito, S.; Soma, M.; Onishi, T.; Tamaru, K. *J. Chem. Soc., Chem. Commun.* **1980**, 543. (b) Domen, K.; Naito, S.; Onishi, T.; Tamaru, K. *Chem. Phys. Lett.* **1982**, *92*, 433. (c) Domen, K.; Kudo, A.; Onishi, T. *J. Catal.* **1986**, *102*, 92.

(2) Kohno, M.; Kaneko, T.; Ogura, S.; Sato, K.; Inoue, Y. *J. Chem. Soc., Faraday Trans.* **1998**, *94*, 89.

(3) Sayama, K.; Arakawa, H. *J. Chem. Soc., Faraday Trans.* **1997**, *93*, 1647.

(4) Sayama, K.; Arakawa, H. *J. Photochem. Photobiol., A* **1996**, *94*, 67.

(5) Domen, K.; Kudo, A.; Shinozaki, A.; Tanaka, A.; Maruya, K.; Onishi, T. *J. Chem. Soc., Chem. Commun.* **1986**, 356.

(6) Kim, H. G.; Hwang, D. W.; Kim, J.; Kim, Y. G.; Lee, J. S. *Chem. Commun.* **1999**, 1077.

(7) (a) Kato, H.; Kudo, A. *Catal. Today* **2003**, *78*, 561. (b) Kato, H.; Asakura, K.; Kudo, A. *J. Am. Chem. Soc.* **2003**, *125*, 3082.

(8) Ikeda, S.; Itani, T.; Nango, K.; Matsumura, M. *Catal. Lett.* **2004**, *98*, 229.

(9) Sato, J.; Saito, N.; Nishiyama, H.; Inoue, Y. *J. Phys. Chem. B* **2001**, *105*, 6061.

(10) Ikarashi, K.; Sato, J.; Kobayashi, H.; Saito, N.; Nishiyama, H.; Inoue, Y. *J. Phys. Chem. B* **2002**, *106*, 9048.

(11) Sato, J.; Kobayashi, H.; Ikarashi, K.; Saito, N.; Nishiyama, H.; Inoue, Y. *J. Phys. Chem. B* **2004**, *108*, 4369.

(12) Sato, J.; Saito, N.; Yamada, Y.; Maeda, K.; Takata, T.; Kondo, J. N.; Hara, M.; Kobayashi, H.; Domen, K.; Inoue, Y. *J. Am. Chem. Soc.* **2005**, *127*, 4150.

(13) (a) Williams, R. *J. Chem. Phys.* **1960**, *32*, 1505. (b) Ellis, A. B.; Kaiser, S. W.; Bolts, J. M.; Wrighton, M. S. *J. Am. Chem. Soc.* **1977**, *99*, 2839.

(14) (a) Hitoki, G.; Takata, T.; Kondo, J. N.; Hara, M.; Kobayashi, H.; Domen, K. *Chem. Commun.* **2002**, 1698. (b) Hitoki, G.; Ishikawa, A.; Takata, T.; Kondo, J. N.; Hara, M.; Domen, K. *Chem. Lett.* **2002**, *31*, 736. (c) Kasahara, A.; Nukumizu, K.; Hitoki, G.; Takata, T.; Kondo, J. N.; Hara, M.; Kobayashi, H.; Domen, K. *J. Phys. Chem. A* **2002**, *106*, 6750.

(15) Maeda, K.; Takata, T.; Hara, M.; Saito, N.; Inoue, Y.; Kobayashi, H.; Domen, K. *J. Am. Chem. Soc.* **2005**, *127*, 8286.
(16) Maeda, K.; Teramura, K.; Masuda, H.; Takata, T.; Saito, N.; Inoue, Y.; Domen, K. *J. Phys. Chem. B* **2006**, *110*, 13107.
(17) Ishikawa, A.; Takata, T.; Kondo, J. N.; Hara, M.; Kobayashi, H.; Domen, K. *J. Am. Chem. Soc.* **2002**, *124*, 13547.
(18) JCPDS Card: No. 38-1374.
(19) Lee, Y.; Watanabe, T.; Takata, T.; Hara, M.; Yoshimura, M.; Domen, K. *J. Phys. Chem. B* **2006**, *110*, 17563.
(20) Shimodaira, Y.; Kudo, A.; Kobayashi, H. *Chem. Lett.* **2007**, *36*, 170.
(21) Linke, W. F. *Solubilities, Inorganic and Metal Organic Compounds*, 4th ed.; Van Nostrand: Princeton, NJ, 1958; Vol. I (A−Ir).